Liquid Crystals
Publication details, including instructions for authors and subscription information:
http://www.informaworld.com/smpp/title~content=t713926090

Elastic, dielectric and optical constants of 4'-pentyl-4-cyanobiphenyl

A. Bogi; S. Faetti

Online publication date: 06 August 2010

To cite this Article Bogi, A. and Faetti, S.(2001) 'Elastic, dielectric and optical constants of 4'-pentyl-4-cyanobiphenyl', Liquid Crystals, 28: 5, 729 — 739
To link to this Article: DOI: 10.1080/02678290010021589
URL: http://dx.doi.org/10.1080/02678290010021589

LIQUID CRYSTALS, 2001, VOL. 28, NO. 5, 729–739

Elastic, dielectric and optical constants of 4′-pentyl-4-cyanobiphenyl

A. BOGI
Dipartimento di Fisica, Via Buonarroti 2, 56127 Pisa, Italy

and S. FAETTI*
INFM and Dipartimento di Fisica, Via Buonarroti 2, 56127 Pisa, Italy

(*Received 4 August 2000; in final form 16 October 2000; accepted 30 October 2000*)

4′-*n*-Pentyl-4-cyanobiphenyl (5CB) is a room temperature nematic liquid crystal with a high positive dielectric anisotropy and a high chemical stability. Many experimental results concerning the elastic and dielectric constants of 5CB are available in the literature, although there is often no satisfactory agreement between the experimental data obtained by different groups, especially as far as the dielectric constants are concerned. Furthermore, no detailed investigation of the temperature dependence of the elastic and dielectric constants close to the nematic–isotropic transition temperature T_{NI} has yet been reported. In this paper, we report the measurement of the elastic and dielectric constants of 5CB, and the temperature behaviour close to T_{NI} has been investigated in detail. The experiment consists in the measurement of the director deformation induced by an electric field using simultaneously both a dielectric and an optical method. The simultaneous use of these two methods provides an indirect check on the reliability of the measurements. Special attention has been devoted to control possible sources of uncertainty. In particular, the effects of finite anchoring energy and of finite pretilt angle have been considered. The temperature dependence of the anisotropy of the refractive indices is also obtained in the experiment.

1. Introduction

4′-*n*-Pentyl-4-cyanobiphenyl (5CB) is a room temperature nematic liquid crystal with a high positive dielectric anisotropy and a high chemical stability. This feature makes 5CB very interesting for fundamental investigations on nematic liquid crystals. For this reason many experimental results on the elastic and dielectric constants of 5CB are available in the literature [1–17]. However, no detailed investigation of these constants close to the nematic–isotropic transition temperature T_{NI} has been reported. In this temperature region the bulk characteristic constants of nematic liquid crystals exhibit a great temperature dependence so that their actual value can hardly be extrapolated from measurements at lower temperatures. Furthermore, there is often no satisfactory agreement between the experimental data obtained by different groups, especially as far as the dielectric constants are concerned. These discrepancies are often much higher than the estimated accuracy of the measurements which is typically of the order of 2%. A possible reason for these discrepancies is the different chemical purity of samples. Indeed, the dielectric permittivity is very sensitive to impurities. Furthermore, in a recent paper Murakami and Naito [8] report that the dielectric constants of 5CB exhibit a slow but appreciable drift (within a month) probably due to injection of impurities from the contacting media (glue, polyimide layers …). This degradation phenomenon too could be a cause of some observed discrepancies.

In this paper, we report an investigation of the elastic and dielectric constants of 5CB with special attention paid to the transition region. The experimental method is based on the investigation of the Fréedericksz transition induced by an electric field [3, 7]. The director distortion is detected by measuring both the capacitance of a nematic cell and the birefringence. The simultaneous use of these two methods provides two independent measurements of the elastic constants and a check on the reliability of the experimental measurements. Special attention has been devoted to the control of possible sources of systematic experimental error. In particular, the influence of finite anchoring energy, of finite pretilt

*Author for correspondence; e-mail: faetti@df.unipi.it

Liquid Crystals ISSN 0267-8292 print/ISSN 1366-5855 online © 2001 Taylor & Francis Ltd
http://www.tandf.co.uk/journals
DOI: 10.1080/02678290010021589

surface angle and of the dielectric surface aligning layer have been taken into account. To reduce greatly possible contributions due to degradation or contamination of the NLC [8], any complete set of measurements has been made using a fresh sample and maintaining the total measurement time within a two day period which is much smaller than the degradation time observed in [8]. Measurements have been repeated on different samples and with different cells to estimate their reproducibility. The experimental results for both the dielectric anisotropy and the elastic constants are in a satisfactory agreement with those obtained by Bradshaw *et al.* [7].

2. The principle of the experimental method

The experimental method is based on the measurement of the response of the nematic liquid crystal to an external electric field [7]. The NLC is sandwiched between two parallel plates covered by thin ITO conducting layers and maintained at a distance d by two spacers. A thin rubbed polyimide layer is deposed on the two plates to induce a planar director orientation with a small pretilt angle θ_p on both the surfaces. An a.c. voltage at a frequency of 3030 Hz is applied to generate an electric field $\mathbf{E}$ along the z-axis orthogonal to the plates. The period of the oscillating signal is much smaller than the characteristic response time of the director field and much smaller than the characteristic relaxation time of ionic charges. Then, the director does not follow the oscillations of the electric field, but reaches a static configuration which depends only on the rms value V of the applied voltage. Furthermore, the nematic liquid crystal behaves as an ideal dielectric medium with no space charges. The director field at a given distance z from one surface is $\mathbf{n} \equiv [\cos\theta(z), 0, \sin\theta(z)]$ where $\theta(z)$ is the angle between the director and the surface plane. For a purely dielectric nematic layer, the dielectric displacement D has to be constant everywhere ($\partial D/\partial z = \rho = 0$) and the bulk free energy density is

$$f = \frac{1}{2}(K_{11}\cos^2\theta + K_{33}\sin^2\theta)\dot{\theta}^2 + \frac{D^2}{2\varepsilon_o(\varepsilon_\perp\cos^2\theta + \varepsilon_\parallel\sin^2\theta)} \quad (1)$$

where K_{11} and K_{33} are the splay and bend elastic constants and $\varepsilon_\perp$ and $\varepsilon_\parallel$ are the dielectric constants orthogonal and parallel to the director, respectively. The equilibrium director angle $\theta(z)$ is obtained by minimizing the total free energy per unit surface area $F = \int_0^d f\,dz + 2W(\theta_s)$, where the anchoring energy function $W(\theta_s)$ and the surface angles θ_s are assumed to be the same at both surfaces of the nematic layer. Using the standard variational approach and looking for an even equilibrium solution one obtains the three equations [18]:

$$\frac{d}{2} = \int_{\theta_s}^{\theta_m} d\theta \left[\frac{1-\gamma\cos^2\theta}{(\cos^2\theta - \cos^2\theta_m)g(\theta,\theta_m)}\right]^{1/2} \quad (2)$$

$$\frac{V}{2} = \frac{D}{\varepsilon_o\varepsilon_\parallel}\int_{\theta_s}^{\theta_m} d\theta \frac{1}{1-\alpha\cos^2\theta} \times \left[\frac{1-\gamma\cos^2\theta}{(\cos^2\theta - \cos^2\theta_m)g(\theta,\theta_m)}\right]^{1/2} \quad (3)$$

$$\Gamma(\theta_s) = -(K_{11}\cos^2\theta_s + K_{33}\sin^2\theta_s)\dot{\theta}_s \quad (4)$$

with $\gamma = (K_{33} - K_{11})/K_{33}$ and $\alpha = (\varepsilon_\parallel - \varepsilon_\perp)/\varepsilon_\parallel$. θ_m is the director angle at the centre of the cell ($z = d/2$) and

$$g(\theta,\theta_m) = \frac{D^2\alpha}{\varepsilon_o\varepsilon_\parallel K_{33}(1-\alpha\cos^2\theta)(1-\alpha\cos^2\theta_m)}. \quad (5)$$

$\dot{\theta}_s$ in equation (4) is the z-derivative of the director angle at the surface with:

$$\dot{\theta}(z) = \left[\frac{1-\gamma\cos^2\theta}{(\cos^2\theta - \cos^2\theta_m)g(\theta,\theta_m)}\right]^{-1/2}. \quad (6)$$

Equation (2) comes from the solution of the bulk Euler–Lagrange equation; equation (3) states that the integral of the electric field is the applied voltage V and equation (4) is the boundary condition for the equilibrium between the elastic surface torque and the anchoring surface torque $\Gamma(\theta_s) = -\partial W(\theta_s)/\partial\theta_s$. For small values of θ_s, the anchoring energy function is well represented by the Rapini–Papoular expression [19]

$$W(\theta_s) = \frac{W}{2}\sin^2(\theta_s - \theta_p) \quad (7)$$

where W is the anchoring energy coefficient. Equations (2)–(4) are a system of three non-linear equations in the three unknown parameters D, θ_s and θ_m which are solved using a numerical iterative algorithm (see for instance [18]). To obtain accurate values of θ_s, θ_m and D, proper care must be devoted to the numerical treatment of the contribution $(\cos^2\theta - \cos^2\theta_m)^{-1/2}$ which diverges at $\theta = \theta_m$. Once parameters D, θ_m and θ_s are obtained from the numerical program, the optical dephasing $\Delta\phi$ between the extraordinary and the ordinary wave for a transmitted monochromatic beam at normal incidence is calculated from

$$\Delta\phi = \frac{4\pi}{\lambda}\int_{\theta_s}^{\theta_m} d\theta \left[\frac{1-\gamma\cos^2\theta}{(\cos^2\theta - \cos^2\theta_m)g(\theta,\theta_m)}\right]^{1/2} \times \left[\frac{n_\perp n_\parallel}{(n_\perp^2\cos^2\theta - n_\parallel^2\sin^2\theta)^{1/2}} - n_\perp\right] \quad (8)$$

where λ is the optical wavelength, and $n_\perp$ and $n_\parallel$ are the ordinary and the extraordinary refractive indices, respectively. At the same time, the effective dielectric

constant $\varepsilon = Dd/(\varepsilon_o V)$ of the nematic layer is calculated from the numerical algorithm. Both these parameters are measured in our experiment. Optical dephasing $\Delta\phi$ is measured using the Senarmont method [20], while $\varepsilon = C/C_o$ is obtained from the measurement of the capacitance C of the NLC layer, where C_o is the empty cell capacitance. From the comparison between the theoretical and experimental behaviours of $\Delta\phi$ and ε versus V, the unknown bulk and surface constants K_{11}, K_{33}, $\varepsilon_\perp$, $\varepsilon_\parallel$, $\Delta n = n_\parallel - n_\perp$, θ_p and W can be obtained if $n_\perp$ and d are known. The dielectric parameter ε is not sensitive to $n_\parallel$ and $n_\perp$, while the optical dephasing $\Delta\phi$ is weakly sensitive to $n_\perp$ but highly sensitive to the product $\Delta n\ d$. Usually, measurements of elastic constants are made with the *a priori* assumption that anchoring is strong ($W \to \infty$) and $\theta_p = 0$. With this assumption, K_{11} is obtained from the measurement of the Fréedericksz threshold voltage [21] $V_{to} = \pi[K_{11}/(\Delta\varepsilon\varepsilon_o)]^{1/2}$, where $\Delta\varepsilon = \varepsilon_\parallel - \varepsilon_\perp$ is the dielectric anisotropy. However, according to Rapini [22], a finite anchoring energy or a finite pretilt angle can affect the threshold voltage and the accuracy of the measurements of the elastic constants. For this reason, we have introduced θ_p as a free parameter and we have made a direct experimental check of the validity of the assumption of strong anchoring using the Yokoyama–van Sprang method [20]. In our experimental conditions, the anchoring contribution is found to be completely negligible and the remaining unknown parameters K_{11}, K_{33}, $\varepsilon_\perp$, $\varepsilon_\parallel$, $\Delta n = n_\parallel - n_\perp$ and θ_p can be obtained with a satisfactory accuracy from the numerical fit of the experimental values of the curves $\Delta\phi(V)$ and $\varepsilon(V)$ with the theory. To reduce greatly the convergence time of the numerical mean square fitting algorithm, it is important to have a first estimation of the unknown parameters. In the following subsection we briefly describe the procedure used to obtain suitable starting values (within 10%) for the free parameters.

2.1. *Preliminary determinations of the unknown bulk constants*

The thickness $d \approx 25\,\mu m$ of the cell gap is measured using an interferometric method with an estimated uncertainty lower than of $0.2\,\mu m$. The ordinary refractive index $n_\perp$ of 5CB is taken from Karat and Madhusudana; the estimated accuracy is better than 0.1% [23]. The other parameters K_{11}, K_{33}, θ_p, $\varepsilon_\parallel$, $\varepsilon_\perp$ and $n_\parallel$ are obtained from the best fit of curves $\varepsilon(V)$ and $\Delta\phi(V)$. A satisfactory starting value for the birefringence Δn is obtained from the measurement of the optical dephasing at zero voltage:

$$\Delta\phi(0) = \frac{2\pi}{\lambda}[n(\theta_p) - n_\perp]d \qquad (9)$$

where

$$n(\theta_p) = \frac{n_\parallel}{\left(\cos^2\theta_p - \frac{n_\parallel^2}{n_\perp^2}\sin^2\theta_p\right)^{1/2}}. \qquad (10)$$

In our experiment $\theta_p \ll 1°$, and $\Delta\phi(0) \approx 2\pi\Delta nd/\lambda$. In the same way, $\varepsilon_\perp$ is obtained from the measurement of the dielectric constant at voltages much lower than the Fréedericksz threshold where $\varepsilon \approx \varepsilon_\perp \cos^2\theta_p + \varepsilon_\parallel \sin^2\theta_p \approx \varepsilon_\perp$. For strong anchoring and at voltages much greater than the Fréedericksz threshold, $\varepsilon(V) \approx \varepsilon_\parallel - a/V$, where a is a constant coefficient. Then, a suitable value of $\varepsilon_\parallel$ is obtained by a preliminary linear fit of $\varepsilon(V)$ versus $1/V$ for $V > 4V_t$. Starting values of the other parameters (θ_p, K_{11} and K_{33}) are obtained by looking at the behaviour of the curves $\Delta\phi(V)$ or $\varepsilon(V)$ close to the Fréedericksz threshold.

Figure 1 (*a*) shows a typical behaviour of the normalized dephasing $\delta = \Delta\phi/\Delta\phi(0)$ versus V close to the Fréedericksz threshold for some values of the pretilt angle θ_p and for a strong anchoring. The full line corresponds to zero pretilt angle. In such a case, the V-derivative of δ has a discontinuity at the Fréedericksz threshold $V_{to} = \pi[K_{11}/(\varepsilon_o\Delta\varepsilon)]^{1/2}$. The main effect of a finite pretilt angle is a small apparent reduction of the Fréedericksz threshold—V_t in place of V_{to} in figure 1 (*b*)—and a finite curvature of the $\delta(V)$ curve. Approximate values of parameters K_{11} and K_{33} can be obtained from a linear fit of the experimental data with $0.9 > \delta(V) > 0.8$ as shown in figure 1 (*b*). The intercept of the straight line with the horizontal line $\delta = 1$ gives a first rough estimate of V_{to} and, thus, of K_{11}. The slope of the straight line is a linear function of $K_{33}/(K_{11}V_{to})$ which is weakly dependent on θ_p and allows us to obtain a preliminary value for K_{33}. The maximum curvature α_{max} of the $\delta(V/V_{to})$ curve for $\theta_p < 3°$ is an almost linear function of $1/\theta_p$ which depends weakly on the other parameters. Then, the measurement of α_{max} provides a satisfactory estimate of θ_p. All these starting parameters are obtained using the

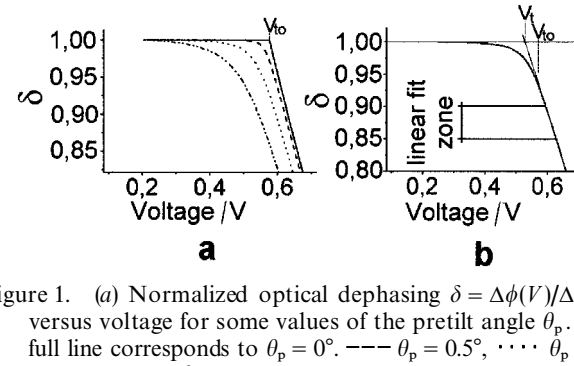

Figure 1. (*a*) Normalized optical dephasing $\delta = \Delta\phi(V)/\Delta\phi(0)$ versus voltage for some values of the pretilt angle θ_p. The full line corresponds to $\theta_p = 0°$. – – – $\theta_p = 0.5°$, · · · · $\theta_p = 2°$ and – · · – $\theta_p = 5°$. (*b*) Definition of the apparent Fréedericksz threshold voltage V_t in the case $\theta_p = 2°$.

same numerical algorithm which performs the successive fits of the experimental data. Note that, in the literature, the elastic constants are usually determined from the measurement of the Fréedericksz threshold with the assumption that the pretilt angle θ_p is zero. This assumption can lead to an underestimate of the elastic constants, as appears evident on looking at figure 1 (*b*) where the apparent threshold V_t is lower than the Fréedericksz value V_{to}. In particular, a pretilt angle $\theta_p = 1°$ leads to a 2% apparent reduction of the Fréedericksz voltage, which corresponds to a 4% apparent reduction of K_{11}.

3. Experimental methods and preliminary observations

In this section we will describe the methods used to obtain the average dielectric constant ε and the optical dephasing $\Delta\phi$ of the nematic liquid crystal.

3.1. *Material, cells and preliminary observations*

The NLC 5CB (K15) was purchased from Merk Ltd. and used without further purification. Different samples have been used in our experiments. The cells used to orient the NLC and to apply the electric field were from the Japanese Company EHC. They are made from two parallel glass plates of thickness 1.1 mm maintained at a distance d ($d \approx 25\,\mu m$ and $d \approx 10\,\mu m$) by two thin spacers. A thin square ITO conducting layer having a $1\,cm^2$ area and a resistivity $50\,\Omega\,cm^{-2}$ is deposited on the two internal plane surfaces of the cell. A thin rubbed polyimide film is deposited on the internal surfaces to induce a homogenous director alignment along the x-axis in the film plane. The Newton interference fringes of the empty cells were observed with monochromatic light in order to select cells having a satisfactory planarity. Cells with a maximum thickness variation lower than 0.5 μm over the whole conducting area were selected. The absolute value of the thickness in the central region was measured by an interferometric method with an uncertainty lower than 0.2 μm. The optical measurements concerned a small portion of the sample ($\approx 4\,mm^2$) where the thickness variation is estimated to be smaller than 0.05 μm. The nematic liquid crystal was introduced into the cell by capillarity and the full cell was observed in the polarizing microscope to control the homogeneity of the alignment and check for the absence of defects both with and without an electric field. Cells exhibiting defects were discarded. The cells were inserted in a thermostat ensuring a temperature stability of 0.002°C and a uniformity of 0.02°C over the whole conducting area. A few measurements very close to T_{NI} were also made using a different thermostatic cell ensuring a stability and temperature uniformity of 0.001°C. The transition temperature T_{NI} was measured by increasing the temperature very slowly starting from 34.9°C and observing the cells in the polarizing microscope. At the transition point, a homogeneous nucleation of isotropic droplets was observed. The coexistence temperature interval of the isotropic and the nematic phase was lower than 0.02°C. T_{NI} is defined here as the temperature in the middle of the coexistence interval. The nematic samples used in the present experiment showed transition temperatures ranging between 35 and 35.1°C.

The clearing temperature of the nematic LC in our cells showed a very small, but continuous decrease with time. This phenomenon is probably the same as that responsible for the dielectric degradation observed in [8] which was interpreted as due to contamination from impurities injected from the polymeric layers and the glue of the cell. In our experiment we found a drift of the transition temperature typically of $0.003°C\,h^{-1}$. This phenomenon could affect the measured temperature dependences of the elastic and dielectric constants, especially close to the clearing temperature. This effect is also evident if one measures the optical dephasing $\Delta\phi(0)$ of the nematic liquid crystal at zero electric field. $\Delta\phi(0)$ is proportional to the anisotropy of the refractive indices which, in turn, is virtually proportional to the scalar order parameter. Then, a reduction of the transition temperature leads to a continuous drift of $\Delta\phi(0)$ which can be easily detected in our experiment (a 0.001°C drift corresponds to a variation of $\Delta\phi(0)$ greater than 0.3° close to T_{NI}). In order to take this drift of T_{NI} into account, we measured $\Delta\phi(0)$ immediately after the measurement of T_{NI} for all the temperatures that would be used in the successive measurements of the dielectric and elastic constants. The entire procedure was made within one hour and provided a calibration table $\Delta T = T_{NI} - T$ versus $\Delta\phi(0)$. The successive measurements on the nematic sample were made setting the temperatures of the thermostat in such a way as to recover the values of $\Delta\phi(0)$ of the calibration table.

3.2. *The experimental methods*

The optical dephasing $\Delta\phi$ is measured using the Senarmont Technique [20]. A schematic view of the optical apparatus is shown in figure 2.

A He-Ne laser beam is separated into two beams I and II by the beam splitter (BS) and the mirror (M). The laser beam is polarized by polarizer P_1 at 45° with respect to the extraordinary axis of the NLC layer (N); it then passes through the nematic layer and a $\lambda/4$ plate with the extraordinary axis parallel to the axis of polarizer P_1. The outgoing beam is linearly polarized at the angle $\delta\phi = \Delta\phi/2$ with respect to the P_1-axis and passes through a rotating polarizer (RP) which rotates at a constant angular velocity $\omega = 10\,rad\,s^{-1}$. Finally it is focused on photodiode Ph1. The output signal of

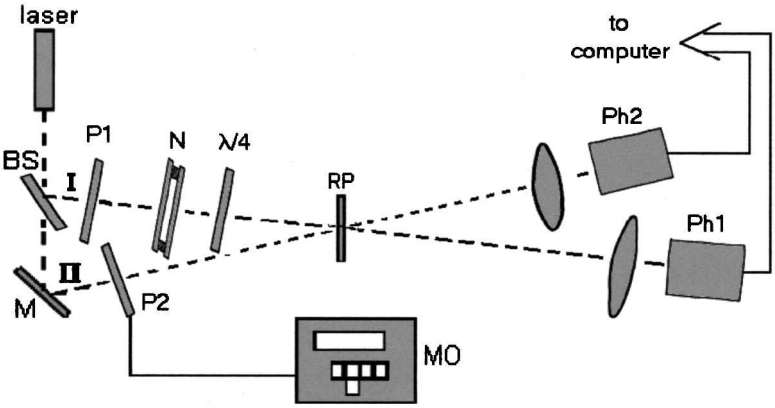

Figure 2. Schematic view of the optical apparatus for the measurement of the optical dephasing $\Delta\phi$ using the Senarmont technique. BS = beam splitter, M = mirror, I = measurement beam, II = reference beam, P1 and P2 = polarizers, N = nematic cell, RP = rotating polarizer, MO = step motor, Ph1 and Ph2 = photodiodes.

the photodiode is:

$$I_1 = A[1 + \cos(2\omega t - \Delta\phi)] \qquad (11)$$

where A is a constant coefficient and $t = 0$ is the time at which the polarization axes of P_1 and RP are parallel. Laser beam II is a reference beam which passes through polarizer P_2 and the rotating polarizer RP and is focused on photodiode Ph2. The output signal $I_2 = B[1 + \cos(2\omega t - \delta)]$ provides an oscillating reference signal with phase δ which can be modified continuously by the rotating polarizer P_2 using the step motor (MO) (minimum step 0.001°). A computer makes a synchronous acquisition of signals I_1 and I_2 during an oscillation period and calculates the Fourier transform at frequency $\omega/2\pi$ and the phase difference $\delta\phi = \Delta\phi - \delta$. δ is set to zero using the procedure below. First, the temperature of the NLC is set to 42°C which is far above the transition temperature T_{NI}. In this condition, the NLC behaves as an isotropic medium with the optical dephasing $\Delta\phi = 0$, and the measured phase difference between I_1 and I_2 becomes $\delta\phi = \delta$. Then, polarizer P_2 is rotated until $\delta\phi$ vanishes. In this way, possible contributions due to the small birefringence of the polyimide layers of the nematic cell (in our experiment $\Delta\phi \approx 1°$) are partially removed and the measured phase difference $\delta\phi$ is due only to the anisotropy of the nematic liquid crystal. The sensitivity of the measurement of the optical dephasing $\Delta\phi$ is 0.01°, while the absolute accuracy is limited by internal reflections and has been estimated to be 0.3° [24].

The electric capacity C of the nematic layer is obtained from the measurement of the real and the imaginary part of the electric impedance Z of the cell. An a.c. oscillating voltage at the frequency 3030 Hz and with a maximum rms value of about 20 V is applied between points A and B of the circuit in figure 3 (*a*) which is put very close to the nematic cell. The cell is connected

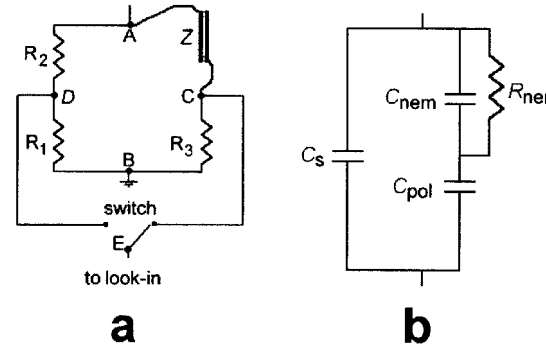

Figure 3. (*a*) Electric circuit used for the measurement of the capacitance of the nematic cell; (*b*) equivalent circuit of the nematic cell. C_s = spurious capacitance due to the connecting wires, C_{pol} = total capacitance of the series of two polyimide layers, C_{nem} = capacitance of the nematic layer, R_{nem} = resistance of the nematic layer.

through two short wires ($\approx$10 cm length) at points A and C. The wires are soldered by indium at the electrodes of the cell to ensure good electric contact. The resistances $R_1 = 100.0\ \Omega$, $R_2 = 136.2\ k\Omega$ and $R_3 = 100\ \Omega$ are chosen such that voltages $V_1 = V(D) - V(B)$ and $V_3 = V(C) - V(B)$ are of the same order of magnitude. The two voltages V_1 and V_3 are alternately sent, using the switch in figure 3 (*a*), to the input of a two-channel digital look-in (Stanford Research Systems SR 830) which measures amplitude and phase of the signals. Due to the low value of resistances R_1 and R_3, the capacity of the long (1.5 m) BNC cable which connects point E to the input of the look-in, the input capacity and resistance of the look-in can be neglected. The real and the imaginary parts of the impedance of the cell are obtained using equation:

$$Z = \frac{V_1 R_3 (R_1 + R_2)}{R_1 V_3} - R_3. \qquad (12)$$

Once the complex impedance of the cell is obtained, the capacitance of the nematic layer is calculated using the equivalent circuit shown in figure 3 (*b*). $C_{nem} = \varepsilon C_o$ is the capacity of the nematic layer and R_{nem} its resistance, where $C_o \approx 35$ pF is the empty cell capacity. C_{pol} is the total series capacitance due to the series of the two orienting polyimide layers, and C_s represents a spurious capacity principally due to the short connecting wires and typically ≈ 1–2 pF. At frequency $\nu = 3030$ Hz, the impedance of our cell is almost entirely capacitive. C_{pol} is expected to be significantly higher than C_o and it gives a very small contribution to the total capacity of the cell. For this reason, the value of C_{pol} has been estimated using thin cells with thickness $d \approx 2\,\mu$m and sufficiently high empty capacity C_o (≈ 400 pF). The impedance Z of these cells was measured with three dielectric fluids of known dielectric constants to obtain the unknown parameters C_s, C_o and C_{pol}. Measurements were repeated with four different cells. We obtained $C_{pol} = 110 \pm 30$ nF. For the nematic cells used in the successive measurements ($d \approx 25\,\mu$m, $C_{nem} \leqslant \varepsilon_{\parallel} C_o \approx 700$ pF) the relative capacitive contribution of the polymeric layer to the total capacitance is almost negligible and it is estimated that $C_{nem}/C_{pol} < 1\%$. Before making mesurements we measured the capacity of an empty cell at the temperatures used for the successive experiments. The empty cell capacity shows a very small increase ($\approx 0.5\%$) when the temperature is increased from 20 to 40°C over a few minutes. This variation of capacity is probably due to a dilation of the spacers or of the polymeric glue, although it shows a complex dependence on the rate of temperature change. The increase in capacity becomes negligible ($< 0.2\%$) if the temperature variation occurs over time greater than a few hours as is the case in our successive experiments.

The introduction in the cell of calibration fluids could leave a few residual impurities on the surfaces of the cell which could produce small defects of the surface director orientation or modify the surface anchoring strength. These effects do not perturb appreciably the measurements of the dielectric constants well below the Fréedericksz transition voltage, but may affect the Fréedericksz threshold behaviour and the measurements of elastic constants. For this reason, the measurements of the director reorientation in the electric field were made without introducing any fluid in the cell, but using the nematic liquid crystal itself as a calibration fluid to obtain the unknown cell parameters C_s and C_o (C_{pol} was set to $C_{pol} = 110$ nF). This procedure requires the preliminary measurement of the dielectric constant of the nematic LC at a low applied voltage ($V \ll V_t$) and at two different temperatures ($T = 25$°C and $T = 38$°C) using cells different from those used in the successive experiments. The dielectric constants measured in these conditions are $\varepsilon_{\perp}(25\text{°C})$ and $\varepsilon_{iso}(38\text{°C})$, respectively. Measurements were repeated with five different cells of thickness $d \approx 25\,\mu$m and their average values were calculated. Parameters C_o and C_s of these cells were obtained using two standard calibration fluids and setting $C_{pol} = 110$ nF. The average measured values were $\varepsilon_{\perp}(25\text{°C}) = 6.6$ and $\varepsilon_{iso}(38\text{°C}) = 11.2$ with an estimated accuracy of 1%. These two dielectric constants together with $C_{pol} = 110$ nF were used to obtain the cell parameters C_o and C_s of the cells used for the successive measurements.

Due to the presence of the thin dielectric polyimide layers in series with the nematic layer, the actual voltage drop V across the nematic layer is slightly lower ($\Delta V < 0.5\%$) than the voltage drop V_{cell} across the cell. Voltage V was calculated exploiting the equivalent circuit in figure 3 (*b*) and using the experimental values of Z, C_o, C_{pol} and V_{cell}.

4. Experimental results

Before starting the experiment, we used the Van Sprang–Yokoyama method [20] to control the validity of the assumption of strong anchoring in our experiment. Points in figure 4 show the normalized optical dephasing δ versus $1/(C_{nem} V)$ well above the Fréedericksz threshold at a temperature $T = T_{NI} - 0.23$°C close to the nematic–isotropic transition. Theory predicts that data are well represented by a straight line and that its intercept with the vertical axis is proportional to $1/W$. Our experimental data are indeed well represented by a straight line which passes through the origin; the anchoring energy is therefore very strong and can be completely disregarded in our experiment.

Figure 5 shows the effective dielectric constant of the nematic layer versus voltage at temperature $T = T_{NI} - 0.23$°C. The thickness of the empty cell is $d = 24.8 \pm 0.2\,\mu$m. Details of the curve close to the Fréedericksz threshold are shown in the inset. The full

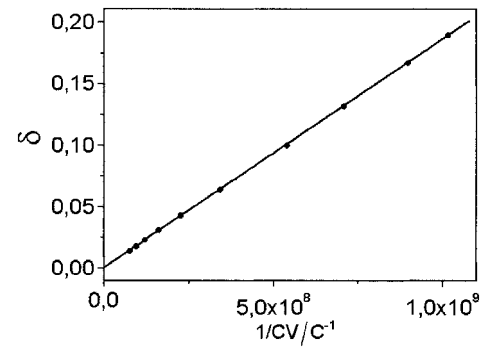

Figure 4. Normalized optical dephasing δ versus $1/(CV)$, where C is the capacitance of the nematic layer and V the applied voltage. Measurements refer to $\Delta T = T_{NI} - T = 0.23$°C. The full line represents the expected behaviour for strong anchoring.

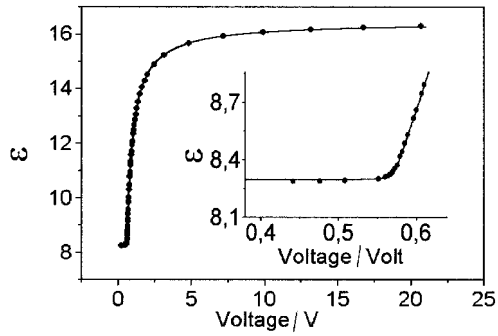

Figure 5. Effective dielectric constant $\varepsilon = C_{nem}/C_o$ of the nematic liquid crystal versus voltage at $\Delta T = T_{NI} - T = 0.23°C$. The behaviour close to the Fréedericksz threshold is shown in the inset. Points correspond to the measured values, while the full line represents the best fit of the experimental data.

line corresponds to the best fit obtained using K_{11}, K_{33}, $\varepsilon_\perp$, $\varepsilon_\parallel$ and θ_p as free parameters and under the assumption of strong anchoring. The curvature close to the Fréedericksz threshold is due to a small pretilt angle $\theta_p = 0.12° \pm 0.01°$.

Figure 6 shows the optical dephasing $\Delta\phi$ at the same temperature for the same cell. A detail of $\Delta\phi$ close to the Fréedericksz threshold is shown in the inset. For any experimental point we expected the attainment of a stationary condition. The full line represents the best fit of the experimental results obtained using K_{11}, K_{33}, $n_\perp$, $n_\parallel$ and θ_p as free parameters and $\varepsilon_\perp$ and $\varepsilon_\parallel$ obtained from the fit of the dielectric data. The best fit algorithm exploits the double precision Fortran subroutine dleamax of the CERN library. Due to the finite electric resistivity ($\rho \approx 10^7\ \Omega$ m) of the nematic layer, some heating could occur especially at the higher applied voltages. To check this point we selected a temperature very close to the nematic–isotropic transition ($T = T_{NI} - 0.05°C$) where all the physical parameters of the nematic liquid crystal depend greatly on temperature. In these conditions we

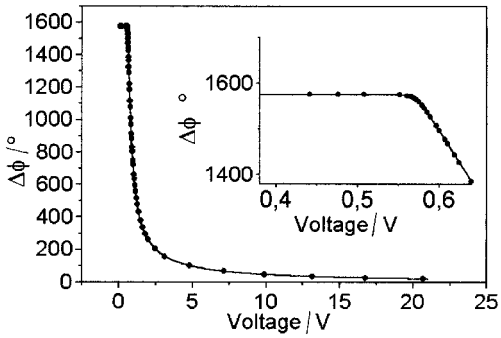

Figure 6. Optical dephasing versus voltage at $\Delta T = T_{NI} - T = 0.23°C$. The behaviour close to the Fréedericksz threshold is evidenced in the inset. Points correspond to the measured values, while the full line represents the best fit of the experimental data.

measured the values of the optical dephasing at a zero electric field. Then, we applied for some time ($\approx$20 min) the maximum electric field ($\approx 1\ V\ \mu m^{-1}$). Finally, the electric field was switched off suddenly and the dephasing was measured. We always found the same optical dephasing measured before the application of the electric field within 0.3° which corresponds to a temperature variation smaller than 1 mK.

Measurements in figures 5 and 6 have been repeated systematically at many temperatures and with three different cells. According to the procedure stated in [3, 7], the final values of the elastic and dielectric constants were obtained from the best fit of the experimental results restricted to the voltage interval V [$0.8V_t$, $2V_t$]. The best fit constants obtained in this way differ less than 0.5% from those which are obtained from a best fit over the whole voltage range.

The dielectric constants $\varepsilon_\perp$, $\varepsilon_\parallel$ and the average dielectric constant $\langle\varepsilon\rangle = (2\varepsilon_\perp + \varepsilon_\parallel)/3$ obtained by the experimental fit of the dielectric measurements are reported in figure 7 versus the temperature difference $\Delta T = T_{NI} - T$. Open circles, crosses and plus signs refer to three different cells. Note that $\langle\varepsilon\rangle = (2\varepsilon_\perp + \varepsilon_\parallel)/3$ is slightly lower ($\approx$1%) than the extrapolated isotropic value (broken line). Many measurements have been made in the interval $0.05°C \leqslant \Delta T < 2°C$ in order to characterize accurately the transitional behaviour. Reproducibility of measurements is better than 0.5% for $\varepsilon_\perp$ and 2% for $\varepsilon_\parallel$ over the whole temperature range. The estimated accuracy is 2% for both these parameters. Each set of measurements with a given cell is well represented (within 0.5%) over the whole investigated temperature

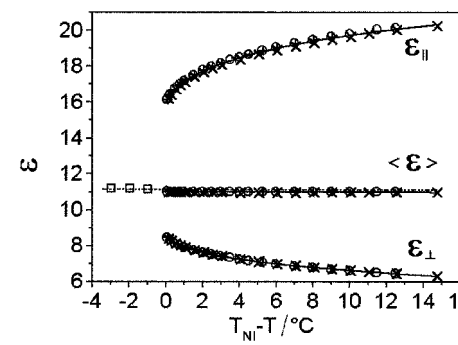

Figure 7. Experimental values of the dielectric constants versus the difference between the transition temperature T_{NI} and temperature T. Three complete sets of measurements with three different cells are represented by the symbols ○, +, ×, respectively. $\langle\varepsilon\rangle$ represents the average dielectric constant in the anisotropic phase. The full line is the best fit of the experimental data with the function ψ in equation (13). The dotted line is the extrapolation of the isotropic values of the dielectric constants at temperatures below T_{NI}.

interval $0.05°C \leqslant \Delta T < 15°C$ by the function

$$\psi = A + B(\Delta T - T_o)^{1/2} + C(\Delta T - T_o) + D(\Delta T - T_o)^{3/2} \quad (13)$$

where $\Delta T = T_{NI} - T$ and A, B, C, D and T_o are suitable coefficients. Then, function ψ provides a useful quantitative representation of the temperature dependence of the experimental data of a single experiment, although it does not correspond to any theoretical model. Coefficients A, B, C, D and T_o change slightly from sample to sample. The values for A, B, C, D and T_o obtained from the best fit of all the experimental points in figure 7 with function ψ are given in table 1.

Other measurements of the dielectric constants of the nematic liquid crystal 5CB have been reported in the literature [1–7]. Experimental data at $\Delta T = 10°C$ and $\Delta T = -3°C$ taken (or extrapolated) from references [1–7] are given in table 2. Data show a somewhat high dispersion, especially as far as the dielectric anisotropy $\Delta\varepsilon = \varepsilon_\parallel - \varepsilon_\perp$ is concerned.

Our experimental values of the dielectric anisotropy are in satisfactory agreement with those obtained by Bradshaw *et al.* [7] using the same method reported here, although there is a small systematic difference as far as the temperature dependence is concerned (see figure 8). Sensibly smaller dielectric anisotropies were reported in all the other papers [1–6]. In these cases (except for [3]), the dielectric constants were obtained using a magnetic field **H** of the order of 1 T to orient the

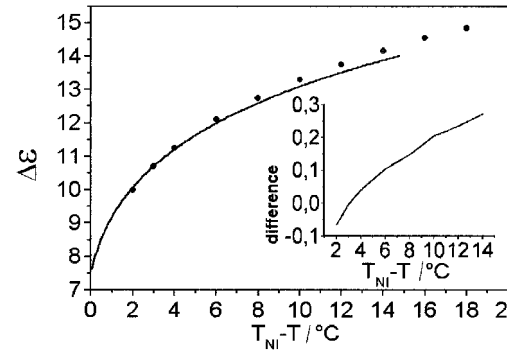

Figure 8. Dielectric anisotropy versus the difference between the transition temperature T_{NI} and temperature T. The full line represents our best fit curve, while points are the experimental values in [7]. The small systematic difference between the results in [7] and our results is shown in the inset.

Table 1. The temperature dependences of the dielectric constants $\varepsilon_\perp$ and $\varepsilon_\parallel$, of the elastic constants K_{11} and K_{33} and of the anisotropy of the refractive indices $\Delta n = n_\parallel - n_\perp$, are represented for the whole investigated temperature range by the empirical function $\psi = A + B(\Delta T - T_o)^{1/2} + C(\Delta T - T_o) + D(\Delta T - T_o)^{3/2}$ where $\Delta T = T_{NI} - T$ denotes the difference between the nematic–isotropic transition temperature $T_{NI} = 35.1°C$ and the measurement temperature T. Coefficients A, B, C, D and T_o that correspond to the bulk constants $\varepsilon_\perp$, $\varepsilon_\parallel$, K_{11}, K_{33} and Δn are reported in the columns of this table.

	Coefficient/SI units				
Parameter	A	B	C	D	T_o/°C
$\varepsilon_\perp$	8.9364	− 1.0786	0.14714	− 0.01156	− 0.16397
$\varepsilon_\parallel$	15.222	1.9544	− 0.19795	0.00843	− 0.16935
K_{11}	1.4017	1.5121	0.004015	− 0.004344	− 0.18335
K_{33}	1.9632	1.3686	0.2911	− 0.02781	− 0.05474
Δn	0.09003	0.03821	− 0.004513	0.0003604	− 0.12483

Table 2. Comparison between our experimental values of the dielectric constants of 5CB and those taken (or extrapolated) from references [1–7] at the same temperatures. $\Delta T = T_{NI} - T$ denotes the difference between the nematic–isotropic transition temperature $T_{NI} = 35.1°C$ and the measurement temperature T. $\varepsilon_\perp$ and $\varepsilon_\parallel$ are the dielectric constants orthogonal and parallel, respectively, to the director for $\Delta T = 10°C$; $\Delta\varepsilon = \varepsilon_\parallel - \varepsilon_\perp$ is the dielectric anisotropy at the same temperature. ε_{iso} represents the dielectric constant in the isotropic phase ($\Delta T = -3°C$).

Data source	$\varepsilon_\perp$ ($\Delta T = 10°C$)	$\varepsilon_\parallel$ ($\Delta T = 10°C$)	ε_{iso} ($\Delta T = 3°C$)	$\Delta\varepsilon$ ($\Delta T = 10°C$)
[1]	6.85	18.4	11.0	11.55
[2]	6.35	17.6	10.6	11.25
[3]	7.7	20.2	11.8	12.5
[4]	6.8	19.5	11.2	12.7
[5]	6.6	17.7	11.2	11.1
[6]	6.5	18.4	11.3	11.9
[7]	—	—	—	13.3
This work	6.6	19.7	11.2	13.15

nematic liquid crystal layer parallel (or orthogonal) to the electric field without previous treatment of the surfaces. The director was assumed to be uniformly oriented along the magnetic field and the dielectric constants $\varepsilon_\perp$ and $\varepsilon_\parallel$ were obtained using the relation $\varepsilon = C_{nem}/C_o$. This procedure is expected to provide experimental values of $\varepsilon_\perp$ and $\varepsilon_\parallel$ which are systematically overestimated or underestimated, respectively, due to the actual presence of two distorted layers of thickness $\xi \approx (K_{ii}/\Delta\chi)^{1/2}/\mathbf{H} = 2\,\mu m$ close to the interfaces [21]. This could explain the lower values of $\Delta\varepsilon$ measured in these experiments. However, the appreciably different values of the isotropic dielectric constant ε_{iso} in [2, 3] (see table 2) suggest that other sources of error are significant. In particular, dielectric constants are expected to be very sensitive to chemical purity, and the observed differences could be due to different chemical purities of the samples. Finally, the degradation effects reported in [8] could also be responsible for some observed differences.

Figure 8 shows the dielectric anisotropy $\Delta\varepsilon$ versus $\Delta T = T_{NI} - T$. The full line represents our results obtained using equation (13) and the coefficients A, B, C, D and T_o given in table 1 for $\varepsilon_\parallel$ and $\varepsilon_\perp$, while the points correspond to the Bradshaw and Raynes results [7]. The small systematic difference between the temperature dependences of the two measurements is brought into evidence in the inset.

To control the reliability of our experimental apparatus we have repeated the measurements of $\varepsilon_\perp(25°C)$ and $\varepsilon_{iso}(38°C)$ using a commercial automatic impedance meter (HP4194A). We obtained a satisfactory agreement with the previous measurements (within 1%). Another independent check on our experimental values of $\varepsilon_\parallel$ was obtained using different cells with the surfaces treated in such a way as to give a homeotropic director orientation [21]. The homogeneity of the homeotropic alignment was controlled using the polarizing microscope. The parallel dielectric constant $\varepsilon_\parallel$ was obtained from the measurement of the capacitance at a low voltage ($V = 0.3\ V_{rms}$) using the formula $\varepsilon_\parallel = C_{nem}/C_o$. Agreement with the values of $\varepsilon_\parallel$ of the full line in figure 7 was found within 1%.

Figures 9 and 10 represent experimental results on the elastic constants K_{11} and K_{33}, respectively, obtained for the three cells. For each cell the two values obtained from the best fit of the dielectric and birefringence data are represented with different symbols. The best fit parameters K_{11} and K_{33} obtained from the birefringence measurements are more accurate. The expected uncertainties on the values of K_{11} and K_{33} with our experimental method are 2% and 5%, respectively [7]. In this case, too, the temperature dependence of each set of experimental data obtained with a single experimental method (dielectric or optical) is well represented (within 0.5% for K_{11} and

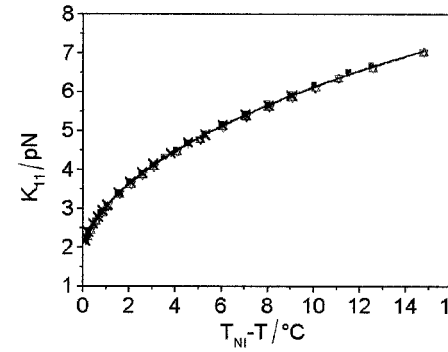

Figure 9. Experimental values of the splay elastic constant K_{11} versus the difference between the transition temperature T_{NI} and temperature T. Experimental results obtained with three different cells are shown in the figure. For each cell and temperature, two different values obtained from the dielectric and optical methods are represented with different symbols. The full line is the best fit of the experimental data with function ψ in equation (13).

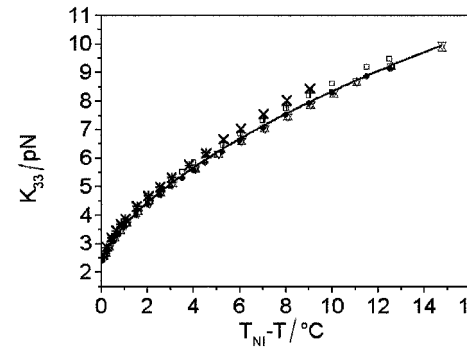

Figure 10. Experimental values of the bend elastic constant K_{33} versus the difference between the transition temperature T_{NI} and temperature T. Experimental results obtained with three different cells are shown in the figure. For each cell and temperature, two different values obtained from the dielectric and optical methods are represented with different symbols. The full line is the best fit of the experimental data with function ψ in equation (13).

1.5% for K_{33}) by function ψ in equation (13). The full lines in figures 9 and 10 represent the best fit of all data using function ψ in equation (13) with the coefficients given in table 1. The different accuracies of the optical and dielectric measurements have been taken into account in making the best fit. Figures 11 and 12 show the experimental results for K_{11} and K_{33} (full line) compared with those reported in the same paper by the two sets of authors, in different laboratories, Bunning and Faber [7] using a magnetic method (full triangles) and Bradshaw and Raynes [7] using the dielectric method (open squares).

A satisfactory agreement between these measurements is obtained. The full lines in the insets in figures 11 and

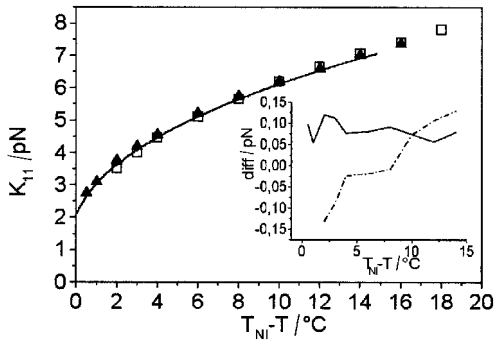

Figure 11. Comparison between our experimental results for the splay elastic constant K_{11} and the Bunning and Faber results [7] (full triangles) and the Bradshaw and Raynes results [7] (open squares). The full line is the best fit of the experimental data with function ψ in equation (13). The full line in the inset is the difference between the Bunning and Faber results and our results; the broken line is the difference between the Bradshaw and Raynes results and our results.

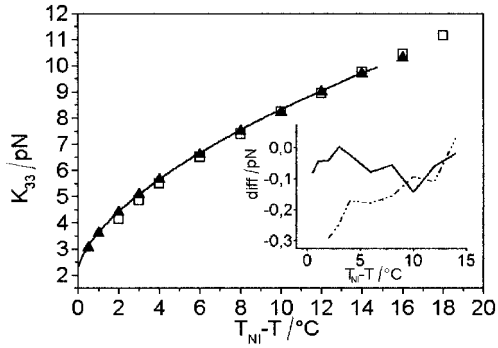

Figure 12. Comparison between our experimental results for the bend elastic constant K_{33} and the Bunning and Faber results [7] (full triangles) and the Bradshaw and Raynes results [7] (open squares). The full line is the best fit of the experimental data with function ψ in equation (13). The full line in the inset is the difference between the Bunning and Faber results and our results; the broken line is the difference between the Bradshaw and Raynes results and our results.

12 represent the difference between the Bunning and Faber magnetic results and our results. The broken lines represent the difference between the Bradshaw and Raynes dielectric results and our results. The small systematic discrepancy on the temperature dependence of the dielectric data is the direct consequence of the analogous discrepancy of the $\Delta\varepsilon$ values in figure 8. A similar kind of discrepancy is present between the magnetic and the dielectric data obtained in [7] by Bunning and Faber and by Bradshaw and Raynes, respectively. These two groups made measurements using the same nematic sample but found appreciably different values for the transition temperatures of this sample (35.6°C and 35.1°C, respectively). According to the authors, this feature suggests the presence of some experimental problem relating to the temperature measurements in one of the two laboratories and could be the main reason for the observed discrepancy on the temperature dependences of the elastic constants. Other authors have made measurements of the elastic constants of 5CB or of the ratio K_{33}/K_{11} [9–17, 25–27] using different experimental methods. Our experimental data for K_{11} are also in satisfactory agreement with those obtained by Coles and Sefton [16] using the electric field dynamic scattering technique and by Hopwood and Coles [14] using the Fréedericksz transition method. Some years ago Hakemi *et al.* [11] measured the optical turbidity of 5CB and found elastic constants much higher than those reported here. More recently [27] Hakemi reanalysed in detail the turbidity measurements and showed that they are greatly affected by the sample geometry. By taking this dependence into account he obtained new values of the elastic constants in satisfactory quantitative agreement with these reported here. Madhusudana and Pratibha [12] obtained elastic constants systematically lower ($\approx$12%) than our values by making measurements of the magnetic Fréedericksz threshold with homeotropic and planar samples. We agree with Bradshaw *et al.* [7] that this difference is probably because the magnetic anisotropy $\Delta\chi$ that Madhusudana and Pratibha used to calculate the elastic constants was not measured, but estimated using an indirect procedure.

Figure 13 shows our experimental results for the anisotropy of the refractive indices at the wavelength $\lambda = 6323$ Å. The uncertainty is estimated to be 1% and is essentially due to the uncertainty on the thickness d of the cell. The full line corresponds to the best fit with function ψ in equation (13) with the coefficients given in table 1. A comparison between our best fit line and

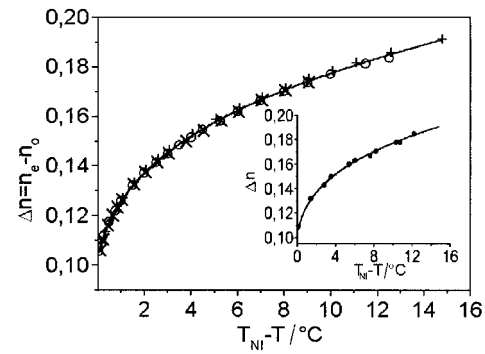

Figure 13. Anisotropy of the refractive indices Δn versus the difference between the transition temperature T_{NI} and temperature T. Experimental results obtained with three different cells are shown in the figure with different symbols. The full lines in the figure and in the inset are the best fits of the experimental data with function ψ in equation (13). Points in the inset represent the experimental values obtained by Karat and Madhusudana [23].

the experimental results by Karat and Madhusudana [23] is shown in the inset. Our results are also in good agreement with the data reported by Horn [28]. The satisfactory agreement of our optical data with those already reported in the literature has an important consequence. Indeed, an important parameter in our experiment is the thickness d of the nematic sample. Our experimental measurements of the thickness d were made using an interferometric method and an empty cell. In principle, due to capillary forces, the thickness of the cell could change when it is filled with the nematic sample. The good agreement between our experimental values of Δn and those of [23, 28] indicates that thickness variations of the cell due to capillary forces are negligible in our experiment. Furthermore, the good agreement between the temperature dependences of Δn with those in [23, 28], also for temperatures very close to the clearing temperature (see the inset in figure 13), gives an indirect proof for the correctness of our temperature measurements.

Finally, the temperature behaviour of the pretilt angle θ_p was also obtained in our experiment. The values of θ_p obtained from our dielectric and optical measurements at each temperature agreed with one another within 0.01°. The pretilt angle has a virtually constant value $\theta_p = 0.09°$ in the temperature interval $1°C < \Delta T < 15°C$ and shows a small increase up to a maximum value $\approx 0.13°$ on approaching the transition temperature T_{NI}.

5. Conclusions

In this paper we have measured the dielectric constants, the splay and bend elastic constants and the anisotropy of the refractive indices of the nematic liquid crystal 5CB. The experimental method was based on the measurement of the dielectric and optical response of the nematic liquid crystal to an electric field. Special care was devoted to investigating in detail the temperature behaviour of these constants close to the nematic–isotropic transition temperature. The contributions of the dielectric aligning polymeric layers, of the anchoring energy and of the pretilt angle are taken into account in our analysis of the experimental data. It has been shown that the anchoring energy is very strong and does not appreciably affect the experimental results. A special effort has been made to maintain the total measurement time as small as possible ($\approx$two days) in order to reduce greatly the degradation phenomena reported in [8]. The reproducibility of the measurements was tested by repeating a complete set of measurements with three different cells. The temperature dependence of each set of data in the investigated temperature interval $0.05°C < \Delta T < 15°C$ is well represented (within 0.5%) by the simple analytical form ψ in equation (13). Our experimental results concerning the dielectric and elastic constants are in satisfactory agreement with the results of Bradshaw *et al.* [7], although a small systematic difference is present as far as the temperature dependences are concerned. The experimental results concerning the anisotropy of the refractive indices are in a good agreement with those reported in [23, 28].

References

[1] Cummins, P. G., Dunmur, D. A., and Laidler, D. A., 1975, *Mol. Cryst. liq. Cryst.*, **30,** 109.
[2] Ratna, B. R., and Shashidar, R., 1977, *Mol. Cryst. liq. Cryst.*, **42,** 185.
[3] Maze, C., 1978, *Mol. Cryst. liq. Cryst.*, **48,** 273.
[4] Jadzin, J., and Kedziora, P., 1987, *Mol. Cryst. liq. Cryst.*, **145,** 17.
[5] Bauman, D., and Haase, W., 1989, *Mol. Cryst. liq. Cryst.*, **168,** 155.
[6] Schell, K. T., and Porter, R. S., 1990, *Mol. Cryst. liq. Cryst.*, **188,** 97.
[7] Bradshaw, M. J., Raynes, E. P., Bunning, J. D., and Faber, T. E., 1985, *J. Phys. (Fr.)*, **46,** 1513.
[8] Murakami, S., and Naito, H., 1997, *Jpn. J. appl. Phys.*, **36,** 2222.
[9] Skarp, K., Lagerwall, S. T., and Stebler, B., 1980, *Mol. Cryst. liq. Cryst.*, **60,** 215.
[10] Bunning, J. D., Faber, T. E., and Sherrel, P. L., 1981, *J. Phys. (Fr.)*, **42,** 1175.
[11] Hakemi, H., Jagodzinski, E. F., and Duprè, D. B., 1983, *J. chem. Phys.*, **78,** 1513.
[12] Madhusudana, N. V., and Pratibha, R., 1982, *Mol. Cryst. liq. Cryst.*, **89,** 249.
[13] Balzarini, D. A., Dunmur, D. A., and Palffy-Muhoray, P., 1984, *Mol. Cryst. liq. Cryst. Lett.*, **102,** 35.
[14] Hopwood, A. I., and Coles, H. J., 1985, *Polymer*, **26,** 1312.
[15] Hara, M., Hirakata, J. I., Toyooka, T., Takezoe, H., and Fukuda, A., 1985, *Mol. Cryst. liq. Cryst.*, **122,** 161.
[16] Coles, H. J., and Sefton, M. S., 1986, *Mol. Cryst. liq. Cryst.*, **3,** 63.
[17] Faetti, S., Gatti, M., and Palleschi, V., 1986, *Rev. Phys. appl.*, **21,** 451.
[18] Stallinga, S., van Haaren, J. A. M., and der Eerenbeemd, J. M. A., 1996, *Phys. Rev. E*, **53,** 1701.
[19] Rapini, A., and Papoular, M., 1969, *J. Phys. Colloq. (Fr.) C-4*, **30,** 54.
[20] Yokoyama, H., and van Sprang, 1985, *J. appl. Phys.*, **57,** 4520.
[21] De Gennes, P. G., 1974, *The Physics of Liquid Crystals* (Oxford: Clarendon Press).
[22] Rapini, A., 1969, PhD thesis, Problemes de surface deus le liquides nemstiques, Faculte de Sciences, Orsey Paris.
[23] Karat, P. P., and Madhusudana, N. V., 1976, *Mol. Cryst. liq. Cryst.*, **36,** 51.
[24] Nastishin, Yu. A., Polak, R. D., Shiyanovskii, S. V., Bodnar, V. H., and Lavrentovich, O. D., 1999, *J. appl. Phys.*, **86,** 4199.
[25] Sharkowski, A., Crawford, G. P., Zumer, S., and Doane, J. W., 1993, *J. appl. Phys.*, **73,** 7280.
[26] Das, M. K., and Paul, R., 1995, *Mol. Cryst. liq. Cryst.*, **259,** 13.
[27] Hakemi, H., 1996, *Mol. Cryst. liq. Cryst.*, **287,** 215.
[28] Horn, R. G., 1978, *J. Phys. (Fr.)*, **39,** 105.